Lead-Acid Battery:

Positive Grid Design Principles

By A. G. CANNONE, D. O. FEDER, and R. V. BIAGETTI

(Manuscript received April 29, 1970)

In this paper, we present accelerated test data which show the superior anodic corrosion and growth behavior of pure lead as compared to lead calcium and lead-antimony positive grids for lead-acid batteries in float service. We relate differences in growth behavior to differences in metallurgy for these three alloy systems. Pure lead has been incorporated into circular grid designs and tests show these to be a substantial improvement over conventional rectangular grids.

A novel grid design concept has been developed and applied to the design of pure lead circular grids. The rate and direction of growth in the grids are controlled by appropriate geometrical design of the grid members. Batteries incorporating these circular grids increase in capacity with age rather than decrease in capacity as do rectangular grids. The circular grids can be designed to provide lifetimes of several centuries.

I. INTRODUCTION

In order to insure that stand-by lead-acid batteries are always in a full state of charge, the batteries are "floated" at 2.17 V per cell which is 110 mV above the open circuit cell potential (O.C. = 2.060 V for 1.210 sp. gr. H_2SO_4). Under these float conditions, PbO_2 is the thermodynamically stable solid phase at the anodes. Consequently, the lead or lead alloy grid is oxidized to PbO_2 . The initial layer of PbO_2 formed on the lead anode is passivating and subsequent corrosion is usually a relatively slow process. The specific volume of PbO_2 is 21 percent greater than that of lead. Therefore, the corrosion product (PbO_2) induces stresses in the lead substrate from which it was formed. The induced stresses cause growth of the grid, which eventually results in failure of the battery. The effect of grid growth is illustrated in Fig. 1 which shows a severely corroded PbCa plate overlayed with a noncorroded grid to show original dimensions. This grid has grown to such an extent that cracking of the PbO_2 pellets and loss of contact with the grid members

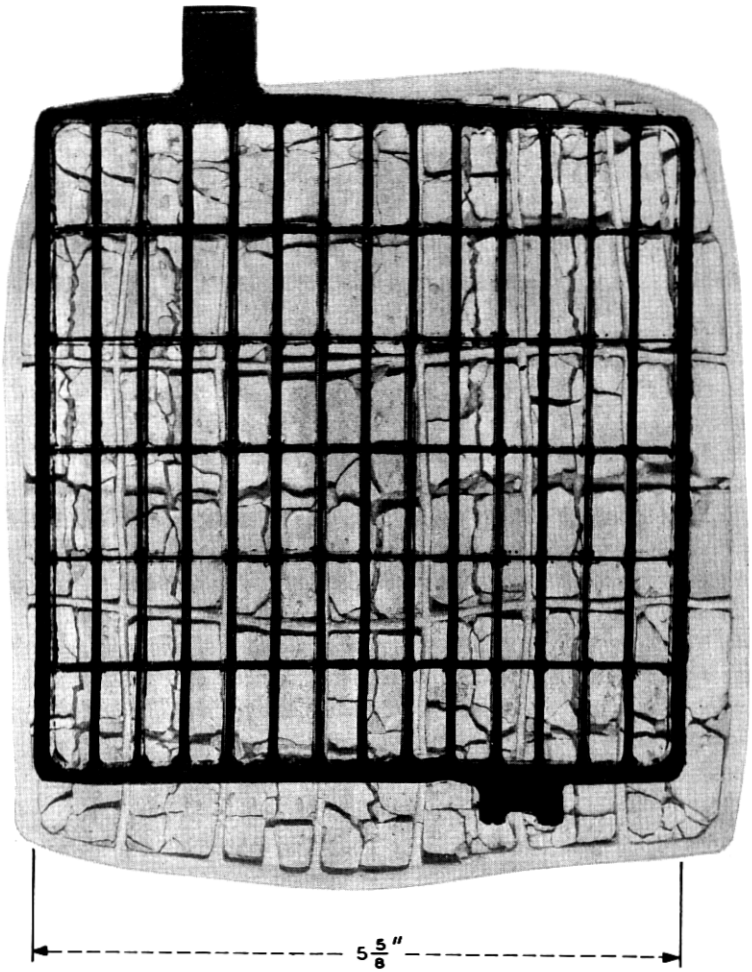

Fig. 1—Severely corroded PbCa grid with overlayed bare grid to show initial dimensions.

have occurred. It is obvious that this must result in a decreased capacity of the plate. Positive plate growth also results in cracking of battery jars, and rupture of jar cover and post cover seals. It was clear that substantial improvements in battery life and performance could be achieved if grid corrosion and growth could be minimized.

It is known that corrosion and growth of PbCa positive grids are

critically related to Ca content.[1,2] Unpublished independent studies by W. W. Bradley and B. A. Cretella, of these laboratories, have shown that the best corrosion behavior of PbCa cells in float service were obtained with cells having low calcium content. This prompted an investigation into the applicability of pure lead for use in long-term, float-service, lead-acid batteries.

Several studies on the anodic corrosion of pure lead have been reported.[3-5] However, these previous investigations are in most cases not relevant to telephone battery float-service conditions and none was of help in predicting the float-service behavior of pure lead versus PbCa and PbSb batteries. Consequently, the anodic corrosion and growth of grids of pure Pb, PbCa and PbSb were compared by using accelerated test procedures which were consistent with our float-service applications.

II. EXPERIMENTAL WORK

The experimental work carried out during this investigation was divided into two phases. The first phase consisted of corrosion and growth studies on pure Pb, PbCa, and PbSb grids of conventional rectangular design (5-5/8″ × 5-7/8″ × 1/4″ thick). This study was designed to establish the validity of the testing procedure and to obtain comparative Pb, PbCa and PbSb performance data. The second phase consisted of accelerated corrosion tests designed to evaluate grid designs and metallurgy developed from results of the first-phase studies.

Corrosion and growth studies were performed on cells assembled in glass jars in 1.210 sp. gr. H_2SO_4. Both pasted plate and bare grid cells were used in this study. Other details of cell construction, such as plate sizes and number of plates, will be given in the appropriate sections of experimental results. Cells were initially given a series of discharge-charge cycles to establish zero time performance after which positive plate dimensions were measured with a micrometer. The cells were then placed at preselected elevated temperatures and the positive plates were potentiostated at 80 mV above the reversible $PbO_2/PbSO_4$ potential at the test temperature. Hg/Hg_2SO_4 electrodes were used for potentiostatic control. Small cells were heated internally with immersion heaters, whereas external box ovens were used for the larger cells. Appropriate thermostats were used for temperature control.

At predetermined intervals the cells were cooled, cycled to establish capacity, measured to determine dimensional changes and returned to hot test.

III. RESULTS AND DISCUSSION

The Phase I experiments utilized commercially available PbCa(0.05 percent Ca) and PbSb (6 percent Sb) grids of a design identical to that shown in Fig. 1. These rectangular grids were received already pasted. Identical design pure lead (99.99 percent) grids were cast in this laboratory using a bottom pour, gravity feed mold. In those cases where pure lead pasted plates were used, these were pasted with a commercially available formulation. All cells tested were 5 plate cells—2 positive plates and 3 negative plates—with appropriately located fiberglass mats and microporous rubber separators.

The test results for PbCa, PbSb and pure Pb are shown in Figs. 2, 3 and 4 respectively where the percent horizontal grid growth is plotted versus time at the various temperatures. The horizontal growth data are those for the midpoints of the positive grids. In most cases, each data point is the average growth of the two grids in a given cell. The superior performance of the pure lead grids is illustrated in Fig. 5 where the growth data is plotted for all three lead systems at 82°C.

The growth of the PbCa and pure Pb grids is quadratically time-dependent, whereas the PbSb data are reasonably linear over the range

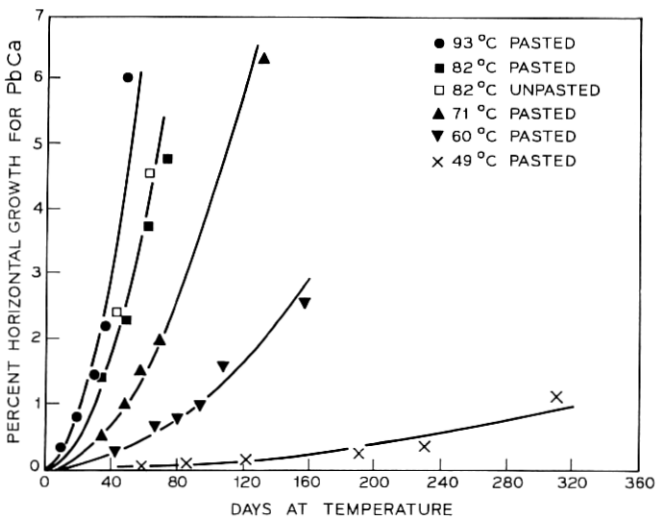

Fig. 2—Percent horizontal growth vs days at temperature for 5-5/8″ × 5-7/8″ × 1/4″ thick PbCa (0.05 percent Ca) grids.

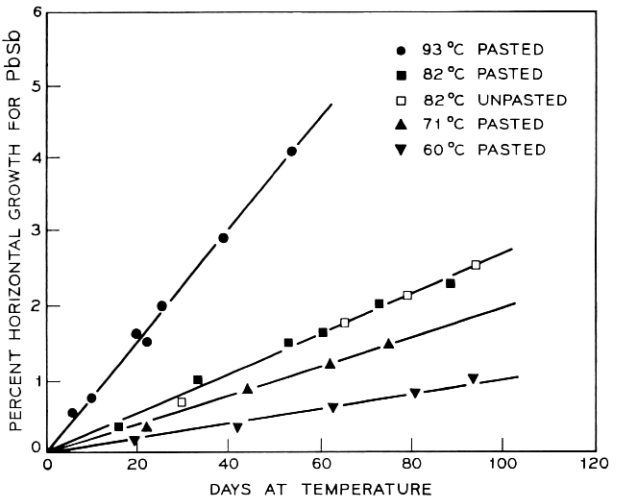

Fig. 3—Percent horizontal growth vs days at temperature for 5-5/8″ × 5-7/8″ × 1/4″ thick PbSb (6 percent Sb) grids.

studied. The curves drawn through the PbCa and pure Pb data points correspond to the equation:

$$\text{Percent Growth} = kt^2 \tag{1}$$

where k is a rate constant and t is time. Curve fitting in accordance with equation (1) was done visually. As can be seen, the curves are a very reasonable fit. The PbSb system shows a linear time dependent growth corresponding to equation (2).

$$\text{Percent Growth} = kt. \tag{2}$$

The temperature dependent rate constants corresponding to equations (1) and (2) are summarized in Table I.

As would be expected, the superior performance of the pure Pb system is also reflected in the ampere-hour capacities of accelerated test cells. Typical behavior is shown in Fig. 6 where the performance of the three Pb systems is shown as a function of time at 93°C. The capacities were normalized in order to eliminate differences in time zero behavior for the three systems. The improved capacity behavior of pure Pb plates may be attributed to the slower growth of pure Pb which enables the grid to maintain contact to the PbO_2 active material for a longer time than for PbCa and PbSb.

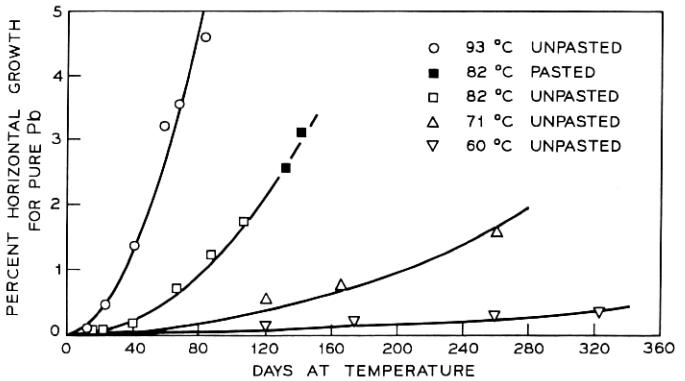

Fig. 4—Percent horizontal growth vs days at temperature for 5-5/8″ × 5-7/8″ × 1/4″ thick pure Pb (99.99 percent) grids.

The reasonable conformance of the PbCa and pure Pb systems to a parabolic growth equation suggests that the growth mechanics for these two systems are similar. Figures 7 and 8 show this to be the case. Corrosion of the PbCa alloy (Fig. 7) is primarily intergranular.[4,6] Figure 8 shows that the corrosion of pure lead is also intergranular. Comparison of Figs. 7 and 8 shows the grain size of the pure lead grid to be considerably larger (approximately 40 times larger) than that of the PbCa grid. This suggests that the superior performance of pure Pb is related to the fewer corrosion sites (grain boundaries) per unit surface area for this system.

3.1 *Room Temperature Behavior*

In order to predict room temperature behavior, a plot was made of log k [equation (1)] versus $1/T$ for the two materials obeying the parabolic growth equation, Pb and PbCa. In the results, shown in Fig. 9, it is seen that the pure Pb grid data follow the Arrhenius law whereas the PbCa data show divergence at 82°C and 93°C. It is known that PbCa is a temperature-sensitive, age-hardening alloy whose metallurgical properties can be altered significantly by heat treatment.[7] The hardness of any given PbCa alloy is determined by the distribution of the Pb_3Ca phase in the alloy. Maximum hardness is associated with uniform distribution and particle size of the Pb_3Ca phase and prolonged heat treatment agglomerates Pb_3Ca which results in a softer alloy. This suggested that the observed anomalies at 82°C and 93°C might be related to changes in PbCa metallurgy induced by testing at these temperatures.

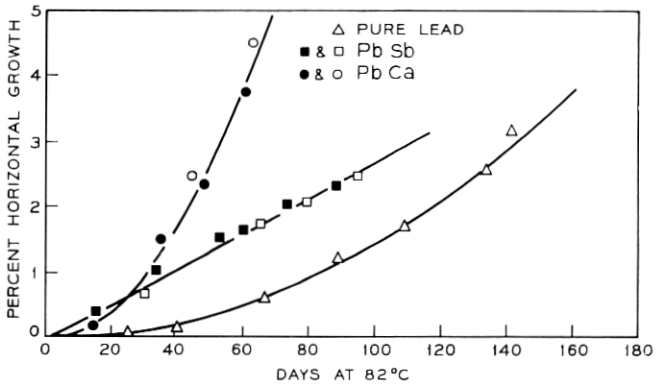

Fig. 5—Percent horizontal growth vs days at 82°C for 5-5/8″ × 5-7/8″ × 1/4″ thick PbCa, PbSb and pure Pb pasted plates.

A second set of accelerated tests on PbCa was carried out in which the grids were heat-treated at 110°C for 11 days prior to testing at elevated temperatures. Accelerated test results on these grids are shown in Fig. 10. Comparison of Figs. 2 and 10 shows that the heat-treated grids grow slower at all temperatures except 93°C. At 93°C the growth curves are essentially the same which indicates that testing at this temperature does indeed induce metallurgical changes in the PbCa system. Figures 11 and 12 are sections of the same PbCa grid before and after heat treatment. There are no obvious differences in grain size or structure which might account for the different growth behaviors. However, tests performed with a Kentron Micro Hardness tester

TABLE I—GROWTH RATE CONSTANTS AT VARIOUS TEMPERATURES FOR $5\frac{5}{8}'' \times 5\frac{7}{8}'' \times \frac{1}{4}''$ THICK PURE Pb, PbSb, PbCa AND HEAT-TREATED PbCa GRIDS

	k^*(%/day^2)			k^{**}(%/day)
T(°C)	Pure Pb	PbCa	PbCa (heat treated)	PbSb
93	7.7×10^{-4}	2.0×10^{-3}	1.9×10^{-3}	7.6×10^{-2}
82	1.5×10^{-4}	1.1×10^{-3}	5.5×10^{-4}	2.7×10^{-2}
71	2.5×10^{-5}	4.2×10^{-4}	9.0×10^{-5}	2.0×10^{-2}
60	4.0×10^{-6}	1.2×10^{-4}	2.0×10^{-5}	1.0×10^{-2}
49		1.0×10^{-5}		

* k in equation (1)—% Growth = kt^2
** k in equation (2)—% Growth = kt

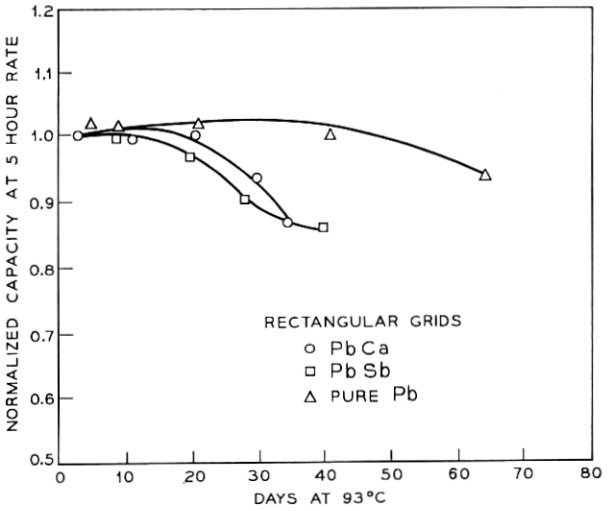

Fig. 6—Normalized 5-hour rate capacities vs days at 93°C for 5-5/8″ × 5-5/7″ × 1/4″ thick PbSb, PbCa and pure Pb grids.

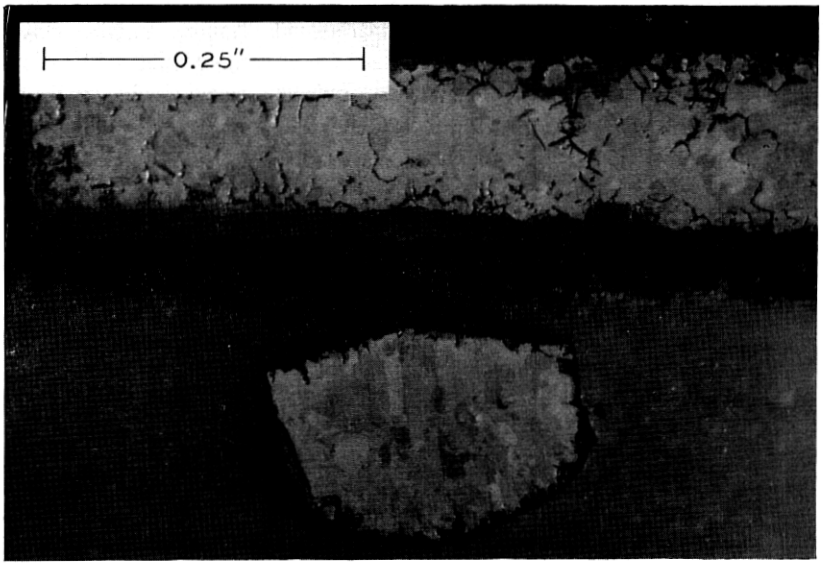

Fig. 7—Section of PbCa (0.05 percent Ca) grid after 36 days at 93°C.

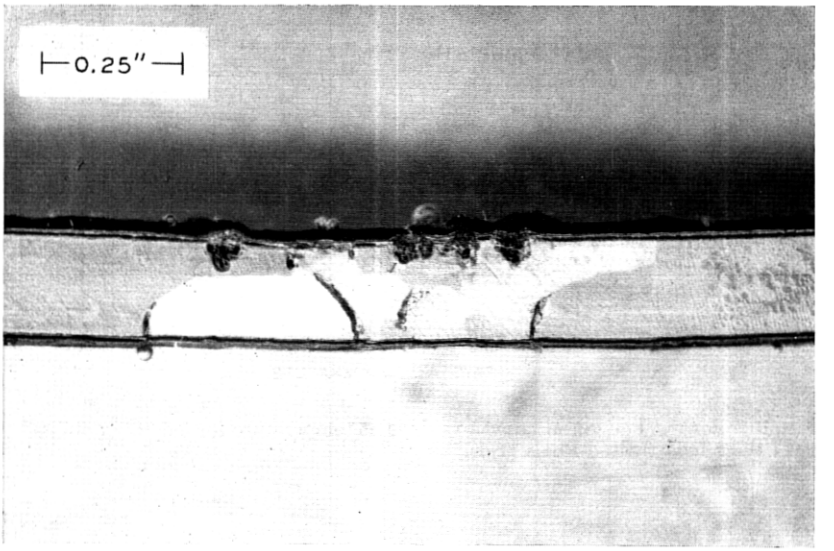

Fig. 8—Section of pure Pb grid after 339 days at 82°C.

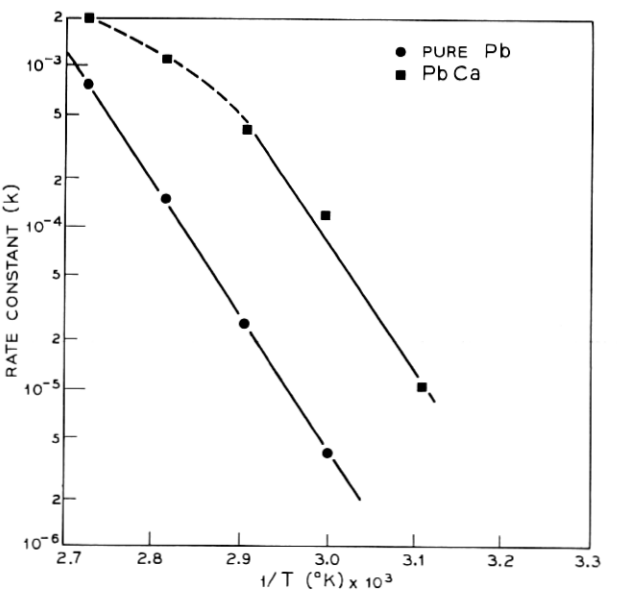

Fig. 9—Rate constant (k) on log scale vs $1/T(°K)$ for 5-5/8″ × 5-7/8″ × 1/4″ thick pure Pb and PbCa.

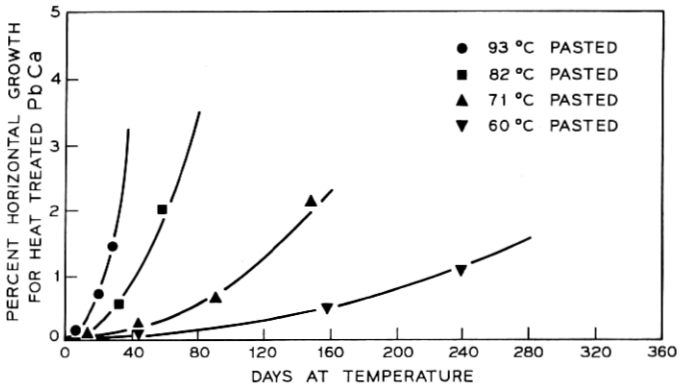

Fig. 10—Percent horizontal growth vs days at temperature for 5-5/8″ × 5-7/8″ × 1/4″ thick heat treated PbCa grids.

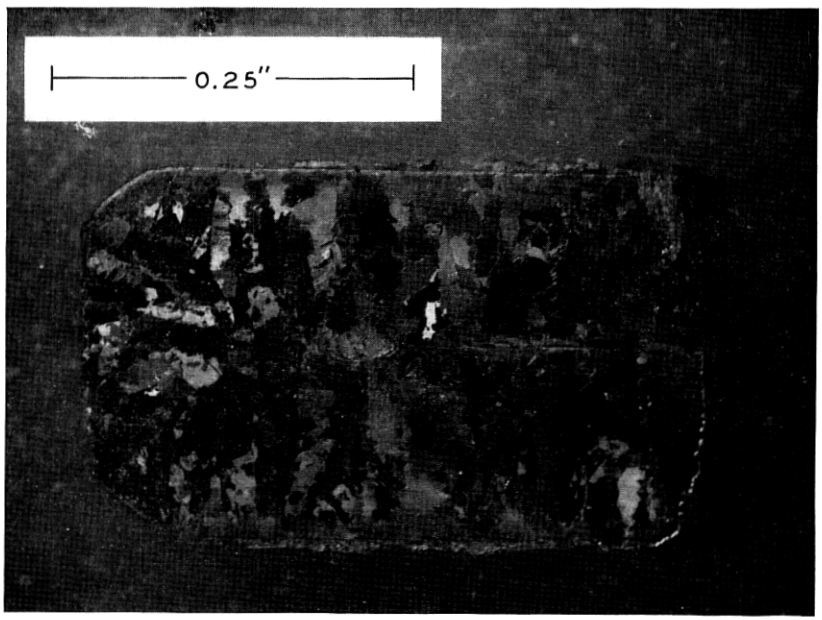

Fig. 11—Section of PbCa (0.05 percent Ca) grid before heat treatment.

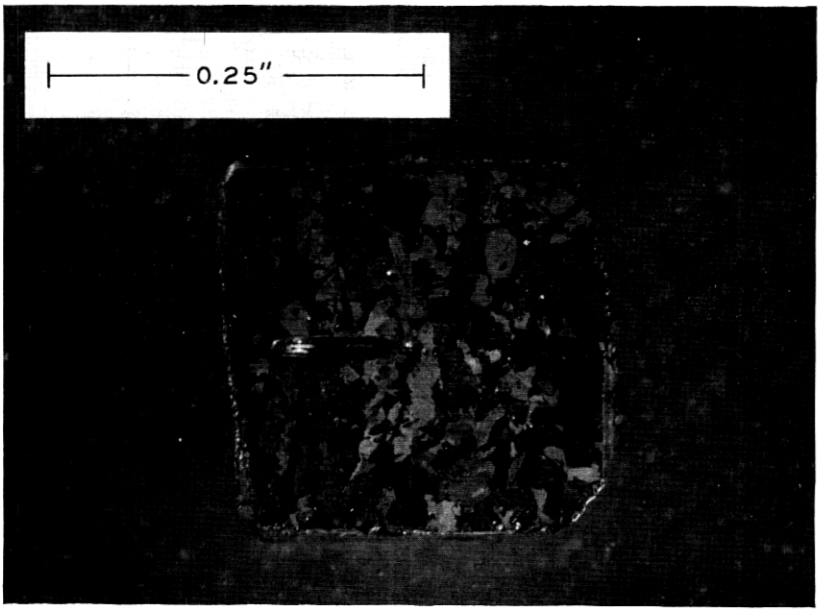

Fig. 12—Section of PbCa (0.05 percent Ca) grid after heat treatment at 110°C for 11 days.

showed the heat treated grids to be somewhat softer than untreated PbCa grids. This is in accord with earlier observations[8] and suggests that the distribution of the Pb_3Ca phase has been altered by heat treatment. It is reasonable to suggest that the corrosion and growth characteristics of PbCa grids are related to the distribution of the Pb_3Ca phase, particularly in the grain boundaries.

Figure 13 shows a log k vs $1/T$ plot for the heat treated PbCa system in addition to the Pb and PbCa data shown in Fig. 9. The data for the heat treated PbCa show Arrhenius behavior indicating that prior heat treatment resulted in stabilization of the PbCa alloy. The rate constant and temperature data for heat treated PbCa are also summarized in Table I. If, as suggested, the growth mechanics are the same for pure Pb and PbCa, then one would expect the slopes (activation energies) of the Arrhenius plots to be the same for these two systems. Figure 9 shows this to be the case with only minor variations.

As mentioned previously, the growth of the PbSb system is linearly time dependent. The fact that the growth behavior for PbSb is different from Pb and PbCa is not unexpected. The PbSb system is more complex

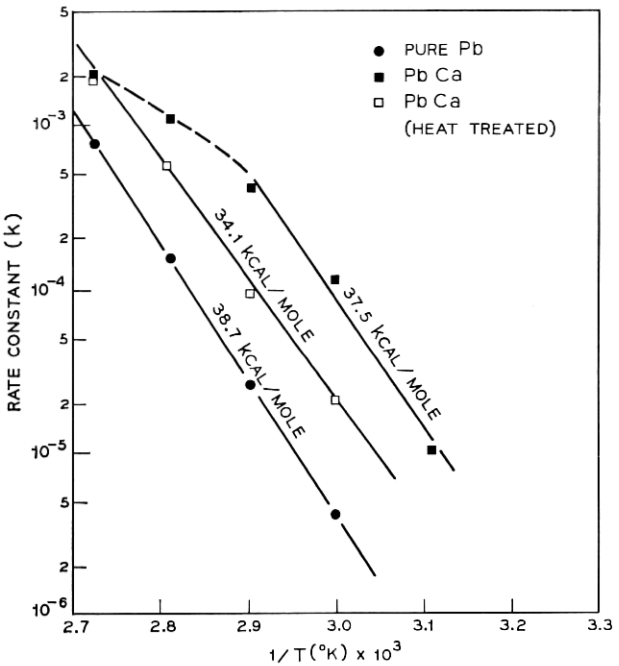

Fig. 13—Rate constant (k) on log scale vs 1/T (°K) for 5-5/8″ × 5-7/8″ × 1/4″ thick pure Pb, PbCa and heat treated PbCa grids.

because corrosion of the alloy is associated with dissolution of Sb. Since Sb is dissolved, it is not incorporated in the PbO_2 corrosion product and the increase in volume resulting from the conversion of Pb to PbO_2 is significantly less for PbSb than it is for pure Pb or PbCa. For example, a 21 percent increase in specific volume occurs in the corrosion of pure Pb to PbO_2 whereas the corresponding increase for 6 percent PbSb is only 9 percent.[9] The log k vs $1/T$ data for the PbSb grids are plotted in Fig. 14.

Room temperature (25°C) rate constants were calculated using the data in Figs. 13 and 14. These are summarized in Table II along with calculated lifetimes to 1 percent (0.056″) and 4 percent (0.225″) growth. Diagnostic studies have shown that 4 percent growth is an approximate upper limit above which the integrity of the battery may be seriously impaired. Table II shows that pure lead would reach 4 percent growth in 82 years whereas the comparable times for PbCa and PbSb are 16.8 and 13.8 years respectively. This should result in a substantial improve-

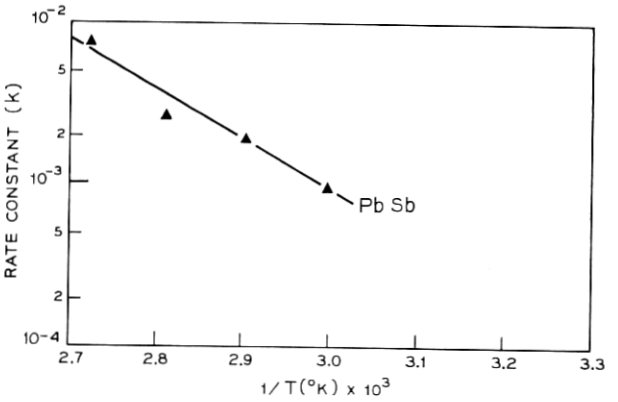

Fig. 14—Rate constant (k) on log scale vs $1/T$ (°K) for 5-5/8″ × 5-7/8″ × 1/4″ thick PbSb grids.

ment in battery life for the pure lead as compared to PbCa and PbSb cells. Heat treatment of PbCa grids is effective in reducing the rate of grid growth. However, heat-treated PbCa is still not comparable to pure lead.

Calculation of room temperature rate constants from Arrhenius plots assumes, of course, that changes in mechanism do not occur at lower temperatures. This has not been substantiated under controlled experimental conditions because of the prohibitively long test times required. However, the calculated 16.8 and 13.8 years room temperature lives to 4 percent growth for PbCa and PbSb respectively are consistent with results obtained from diagnostic studies of cells in field use. In view of this, it is reasonable to assume that the calculated 82 years would be realized by the pure Pb cells in field use.

TABLE II—GROWTH RATE CONSTANTS AT 25°C FOR $5\frac{5}{8}'' \times 5\frac{7}{8}'' \times \frac{1}{4}''$ THICK PURE Pb, PbSb, PbCa AND HEAT TREATED PbCa GRIDS

	k at 25°C	Time to 1% Growth (Years)	Time to 4% Growth (Years)
Pure Pb	$4.41 \times 10^{-9}\%/\text{day}^2$	41	82
PbCa	$1.06 \times 10^{-7}\%/\text{day}^2$	8.4	16.8
PbCa (heat treated)	$4.60 \times 10^{-8}\%/\text{day}^2$	12.8	25.6
PbSb	$7.96 \times 10^{-4}\%/\text{day}$	3.4	13.8

3.2 *New Cell Designed*

In order to capitalize on the superior corrosion and growth behavior of pure Pb, a new cell was designed with a self-supporting interlocking structure to minimize the stress on the soft Pb.[10] This section discusses the design and performance of the conical grids which have been developed for the new cell. Figure 15 shows the first (Design "A") of a series of pure lead positive grid designs that were evaluated. The circular grid (10.9″ O.D. × 0.25″) consists of a series of concentric hoops interconnected by both continuous and interrupted radial members. In this circular design, corrosion and growth should cause the diameters of the concentric hoops to increase. The radial members would be buckled as a result of growth.

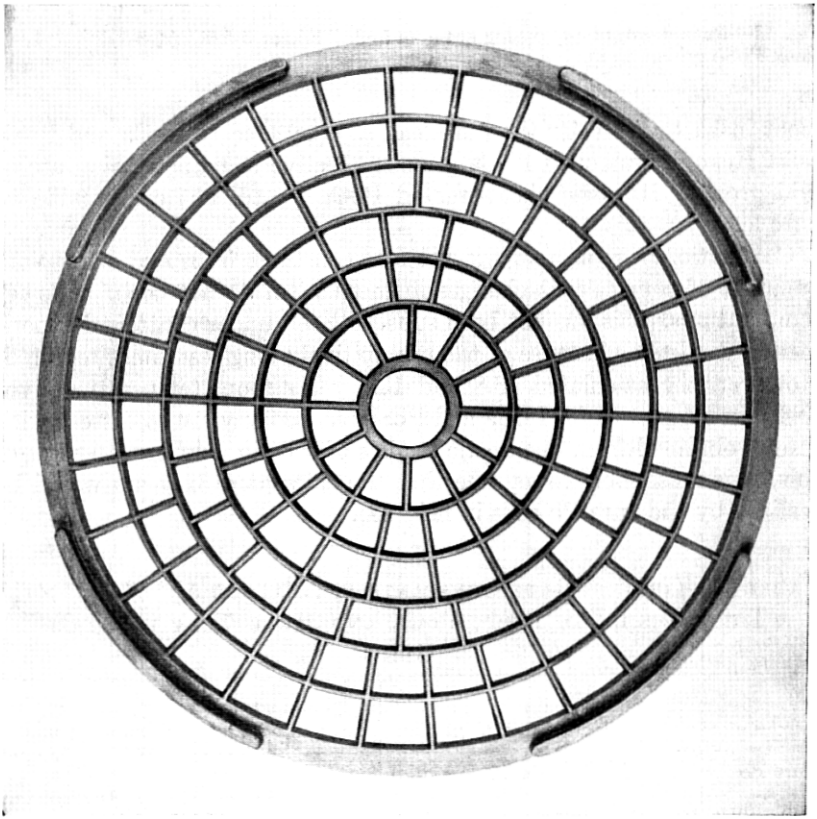

Fig. 15—Design "A" pure Pb grid – 10.9″ O.D. × 0.25″.

Figure 16 shows a different embodiment of this circular grid design concept. This spiral grid (Design "B", 10.9" O.D. × 0.25") has the hoops and radial members prebuckled in an attempt to control the direction of growth of all the members.

Accelerated tests of these positive grid designs were carried out with 160 AH cells (5 hr. rate)—3 positive plates, 4 negative plates. In cells, these grids are shaped to a 10° cone and stacked pancake fashion one atop another. Other details of cell construction are given elsewhere.[10] Results of growth studies for these two grid designs are summarized in Figs. 17 and 18.

The growth data for these two circular designs are roughly linear with time. Since the mechanism of growth is a property of the material and not of grid geometry, growth having quadratic time dependence similar to the rectangular grids was expected. The reason for non-conformance to parabolic growth became apparent after test completion when the cells were disassembled and the grids examined. Figure 19 shows a design "A" grid after 169 days at 93°C. Considerable "mushrooming" has occurred which has substantially distorted the grid from its original 10° conical shape. Other studies showed this same "mushrooming" effect also occurring in the design "B" grids. It was clear that "mushrooming" was the result of unbalanced grid designs in that

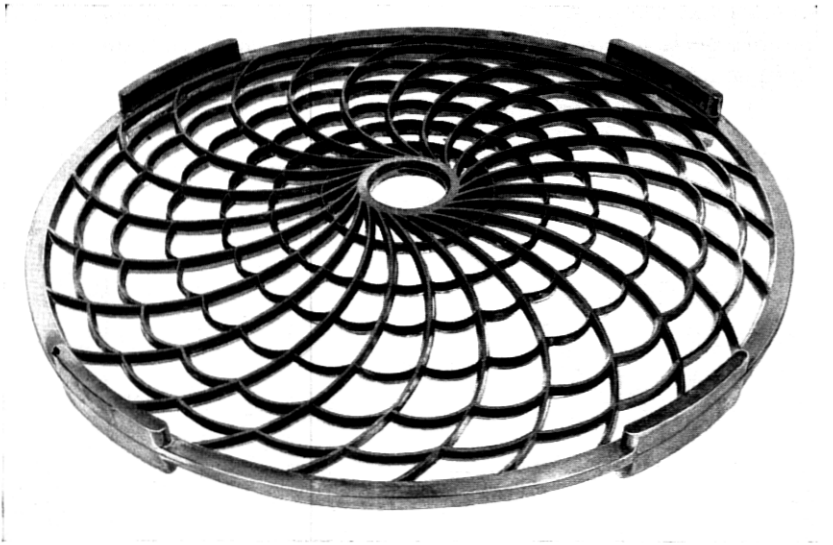

Fig. 16—Design "B" pure Pb grid — 10.9" 0.D. × 0.25".

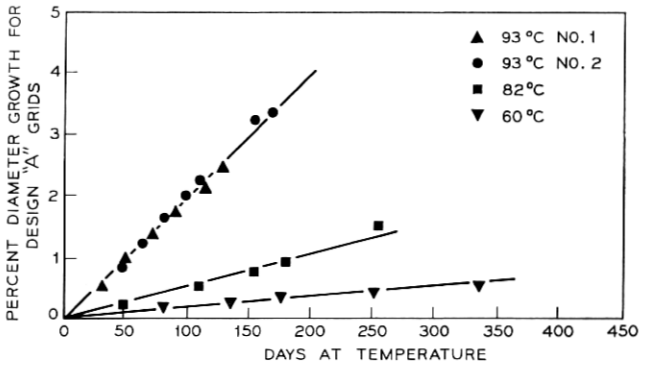

Fig. 17—Percent growth of diameter vs days at temperatire for design "A" pure Pb circular grids.

all the circular hoops were not growing at the same rate. Most of the inner hoops for both grid designs were growing at a faster rate than the outer ring which eventually leads to severe distortion from the original 10° cone.

Evaluation of growth data from the rectangular PbCa grid experiments revealed that the growth of any given member was directly proportional to the surface area (S.A.) and inversely proportional to the cross-sectional area (C.A.) of the member. In effect, the rate constant (k) in equation (1) is a product of two constants, k_1k_2 :

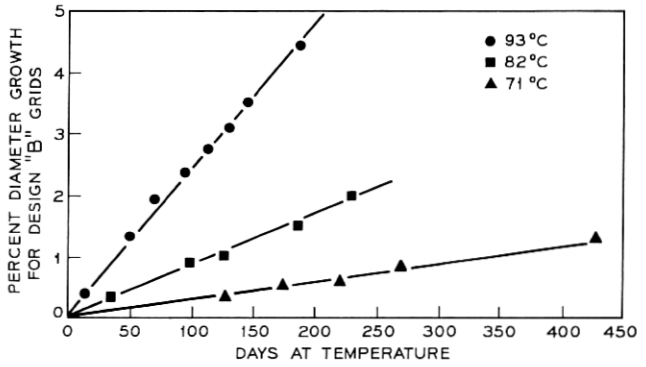

Fig. 18—Percent growth of diameter vs days at temperature for design "B" pure Pb circular grids.

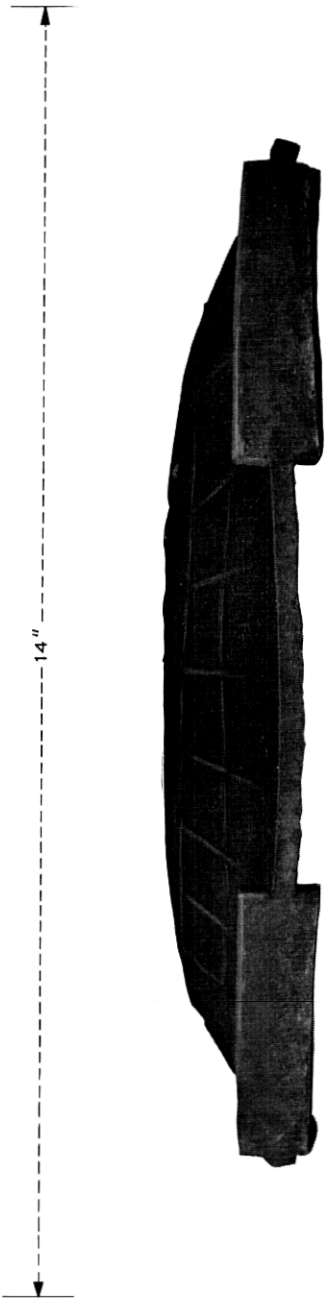

Fig. 19—Design "A" pure Pb circular grid after 169 days at 93°C.

$$\text{Growth} = k_1 k_2 t^{2*} \tag{3}$$

where k_1 is the rate constant for growth and is a function of only the particular alloy system and k_2 is the S.A./C.A. ratio of a grid member. This concept is further clarified by the data in Table III. In Table III, k_1 [equation (4)] is calculated from detailed growth data (PbCa 82°C) on the three different types of rectangular grid member geometries (Fig. 1).

$$k_1 = \frac{\text{Growth}}{k_2 t^2}. \tag{4}$$

TABLE III—GROWTH RATE CONSTANTS AT 82°C FOR VARIOUS GRID MEMBERS OF THE $5\frac{5}{8}'' \times 5\frac{7}{8}'' \times \frac{1}{4}''$ THICK PbCa GRID

k_1(in/day^2)	Growth at 68 Days (inches)	k_2(S.A./C.A.)
8.7×10^{-8}	.008	19.9
8.8×10^{-8}	.013	32.0
8.6×10^{-8}	.021	53.0

It is seen in Table III that k_1 is essentially independent of grid member geometry. The conclusion is that growth data obtained on a member of a given geometry enables one to calculate the growth expected for a large variety of geometric shapes provided the alloy system remains constant. Using this approach, the expected growth of the outer ring of the pure lead design "A" grid was calculated and compared to actual growth at 93°C. Figure 20 shows the measured growth to be significantly greater than that calculated. The reason for this lies in the peculiarities of the grid design which leads to "mushrooming." Table IV lists the S.A./C.A. ratios for each of the rings in the "A" design. Since all the ratios are different, the expected rate of growth for each ring would also be different. Table IV also indicates that the three rings closest to the outer ring would grow faster than the outer ring.

It is suggested that during the initial stages of growth, the faster growth of these inner rings is transmitted via the PbO_2 pellets to the outer ring. This in effect stretches the outer ring resulting in growth larger than would be expected in the normal course of corrosion. During the intermediate stages of growth, the faster growing inner rings eventually lead to distortion from the original 10° plane resulting in the observed mushrooming. During advanced stages of inner ring growth,

* Note that equation (3) expresses growth on an absolute basis rather than the percent basis used previously.

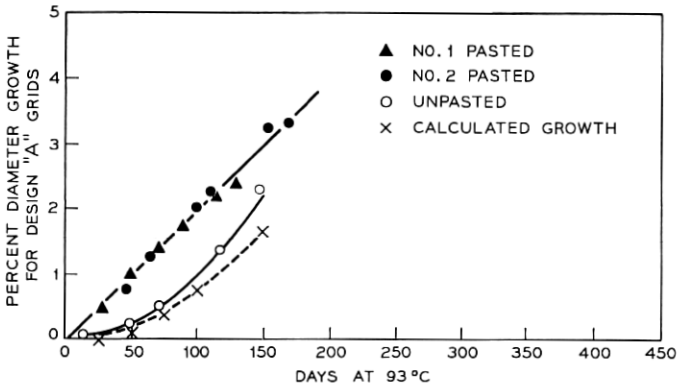

Fig. 20—Experimental and calculated design "A" grid growth vs days at 93°C.

"mushrooming" has become severe and transmission of growth via the PbO_2 paste material is not as effective.

The transmission of growth via the PbO_2 paste material was substantiated in an unpasted grid experiment also shown in Fig. 20. In this case, there is no PbO_2 paste material for transmission of inner ring growth to the outer ring and the growth data correspond much better to that calculated. The growth data given for the "A" and "B" designs represent, therefore, second-order effects controlled by the growth characteristics of the inner ring members of these grids and thus these do not follow the parabolic growth equation. The data, however, still have physical significance and the linear rate constants have been summarized in Table V and plotted in Fig. 21.

The extrapolated 25°C rate constants are 4.62×10^{-5} percent/day and 1.29×10^{-5} percent/day for the "A" and "B" designs respectively. These yield calculated room temperature lives to 4 percent growth

TABLE IV—RATIOS OF SURFACE AREA TO CROSS-SECTIONAL AREA FOR RING SECTIONS OF DESIGN "A" GRIDS

Ring No.	S.A./C.A.
inner	70
2	219
3	331
4	442
5	546
6	657
outer	410

TABLE V—GROWTH RATE CONSTANTS AT VARIOUS TEMPERATURES FOR "A" AND "B" DESIGN PURE LEAD GRIDS

	k^*(%/day)	
T°(°C)	Design "A"	Design "B"
93	2.0×10^{-2}	2.5×10^{-2}
82	5.4×10^{-3}	8.8×10^{-3}
71	—	3.0×10^{-3}
60	1.4×10^{-3}	

k^* corresponds to linear growth equation (% Growth = kt).

(0.420″) of 238 years for the "A" design and 854 years for the "B" design. It is clear that the use of pure lead in a circular design (even though the design is unbalanced) provides positive plates which will not fail as a result of grid growth for extremely long periods of time provided that the ratio of surface area to cross-sectional area of the rings is sufficiently small.

3.3 *Third Circular Design*

In order to overcome the "mushrooming" problem, a third circular grid was designed in which all the circular hoops were balanced such

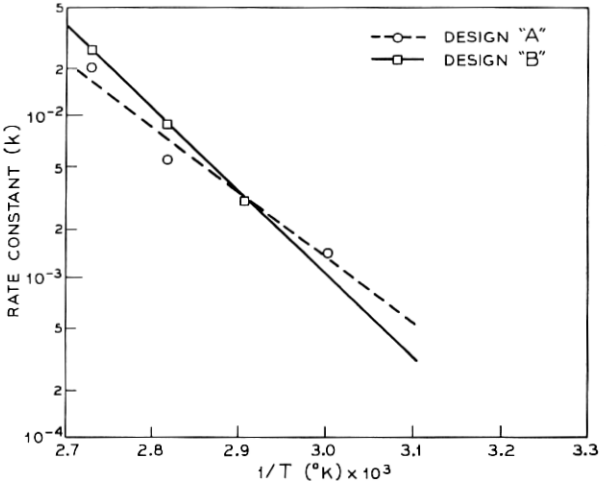

Fig. 21—Rate constant (k) on log scale vs 1/T(°K) for "A" and "B" circular pure Pb grid designs.

that they would all grow at the same rate. Since k_1 in Equation (3) is constant for a particular lead alloy system, a balanced circular grid design is obtained by maintaining k_2 (S.A./C.A.) constant for the hoops. Such a balanced grid design is shown in Fig. 22 (10.9″ O.D. × 0.25″) wherein all the circular sections have the same S.A./C.A.—410 in this case. The S.A./C.A. ratio of 410 is the same as that for the outer rings of the "A" and "B" designs. Figure 23 shows the results of 93°C testing on four cells incorporating this "C" design. There is reasonably close correspondence between the data and the calculated behavior for this design. The growth data show some curvature indicating quadratic time dependence as would be expected on the basis of the results obtained on the rectangular grids. However, the growth data do not conform to a simple parabolic expression [equation (1)]. It may be that the accelerated tests have not yet progressed far enough in time for growth behavior conforming to equation (1) to become obvious. Only 93°C data is available for this design and, consequently, Arrhenius treatment to obtain room temperature performance is not possible. However, comparison of the design "C" data with 93°C data of other pure lead grid designs shows the performance of the "C" design to be superior. For

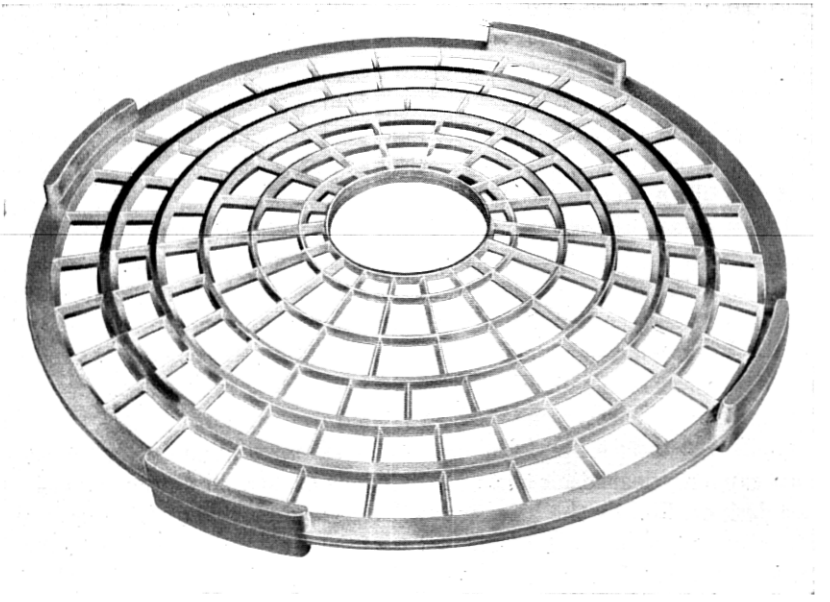

Fig. 22—Design "C" pure lead grid — 10.9″ O.D. × 0.25″.

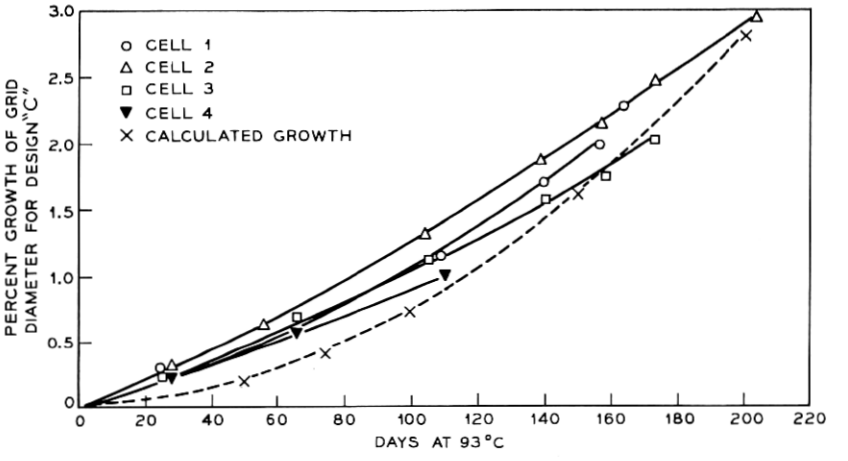

Fig. 23—Percent growth of diameter vs days at 93°C for design "C" pure Pb circular grids.

example, the time to 2 percent growth at 93°C ranges between 148–172 days for design "C" whereas the comparable times are 100, 85, and 50 days for "A", "B" and rectangular designs respectively. Examination of "C" design grids after 93°C testing shows no evidence of "mushrooming" which indicates that this design is indeed balanced. Figure 24 shows a typical "C" plate after 204 days at 93°C. It is seen that the plate is still in excellent condition.

The effects of these various designs and metallurgies are dramatically summarized in Fig. 25. The superior performance of pure lead over PbCa and PbSb in the rectangular design is shown again as it was in Fig. 6. For the "A" and "B" designs the cell capacities increase substantially as corrosion and growth occur. Since the corrosion product is PbO_2, increasing capacity would be expected for grid designs in which contact to the active material was maintained during growth. The capacities of the "A" and "B" designs reach maxima and then degrade. This capacity degradation is a consequence of "mushrooming" for these two designs. Finally the balanced "C" design shows gradually increasing capacity with no maximum reached as of yet. It is reasonable to conclude that capacities of cells made with balanced circular pure lead grids will increase with age rather than decrease as is the case with conventional rectangular cells.

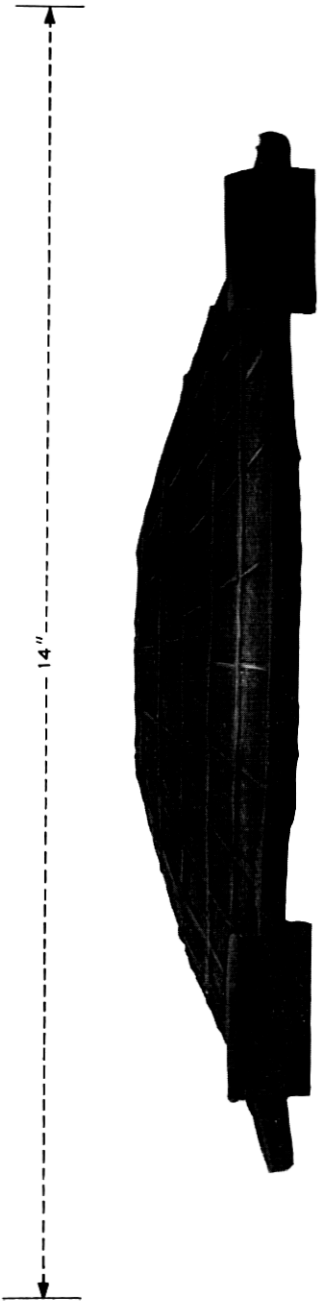

Fig. 24—Design "C" grid after 204 days at 93°C.

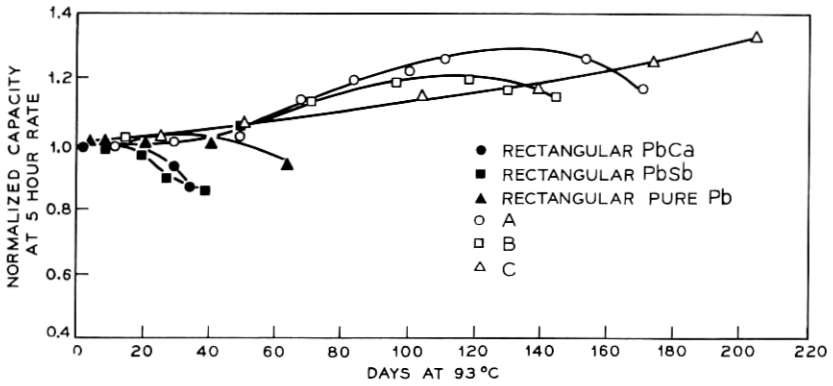

Fig. 25—Normalized 5-hour rate capacity vs days at 93°C for various grid designs.

IV. SUMMARY AND CONCLUSIONS

Accelerated test data show the superior anodic corrosion and growth behavior of pure Pb as compared to the Ca and Sb alloys when used for positive grids in lead-acid cells for float service. The differences in growth behavior are related to the differences in metallurgy for these three alloy systems. Predicted room temperature lifetimes to 4 percent growth are 82, 16.8 and 13.8 years respectively for pure Pb, PbCa and PbSb rectangular grids.

Similar tests on two pure Pb circular grid designs ("A" and "B") show these to be substantially improved over the conventional rectangular designs. Even though both these designs "mushroom" during corrosion and growth, 238 and 854 years were predicted as the room temperature lifetimes to 4 percent growth for the "A" and "B" designs respectively.

Detailed analyses of the growth behavior of both rectangular and circular grids revealed that rate of growth of a grid member was related to the particular geometry of the member and that "mushrooming" of the circular grid designs resulted from unequal growth of the grid members. This analysis led to the development of a novel circular grid design concept wherein the rate and direction of growth could be controlled by proper sizing of the members. This concept was incorporated into the "C" design grid wherein all the circular members have a fixed surface area to cross-sectional area ratio of 410. Tests on cells incorporating this "C" design have verified the expected improved growth and capacity behavior. It is expected that the "C" grid design

will perform satisfactorily for several centuries. In view of the 30-year design life objective for the new Bell System circular lead-acid battery design,[10] it is clear that the "C" grid design easily meets this objective.

Confidence in the expected room temperature behavior of the "C" design has led to the design of another pure lead circular grid. In this newest design, the S.A./C.A. ratio for the circular members has been increased to 600 as compared to 410 for the "C" design. It is expected that this newest design will grow at an absolute rate approximately 1.5 times faster than the "C" design. This "faster" growing grid is more consistent with the design life objective and also provides a reduction in the amount of lead per unit grid volume. Accelerated growth testing of this new design is being initiated and results will be reported at a later date.

V. ACKNOWLEDGMENTS

The authors wish to express their gratitude to those many individuals who have contributed to this manuscript. Special thanks to Messrs. R. A. Landwehrle, P. J. Zsadanyi and J. I. Mount, who were largely responsible for maintenance of the tests, and to Miss M. M. Cook and Mrs. J. R. Hurd for computer handling of the data.

REFERENCES

1. Thomas, U. B., Forster, F. T., and Haring, H. E., "Corrosion and Growth of Lead-Calcium Alloy Storage Battery Grids as a Function of Calcium Content," Trans. Electrochem. Soc., *92* (1947), pp. 313–325.
2. Turner, D. R., and Insinga, L. P., "The Effects of Calcium Content in Lead-Calcium Alloy Grids on the Performance of Lead-Acid Storage Batteries," Abstract No. 33 Electrochem. Soc. Meeting, Oct. 10–14, 1965, Buffalo, N. Y.; published in *Extended Abstracts of Battery Division*, Volume 10, Ann Arbor, Mich.: Electrochem. Soc., 1965, pp. 87–88.
3. Lander, J. J., "Anodic Corrosion of Lead in H_2SO_4 Solution," J. Electrochem. Soc., *98*, No. 6 (June 1951), pp. 213–219.
4. Lander, J. J., and Burbank, N., "Positive-Grid Corrosion in the Lead-Acid Cell: Corrosion Rates of Tin Alloys and the Effect of Acid Concentration on Corrosion," Naval Research Laboratory Report 4076, November 7, 1952.
5. Lander, J. J., "Further Studies on the Anodic Corrosion of Lead in H_2SO_4 Solutions," J. Electrochem. Soc., *103*, No. 1 (January 1956), pp. 1–8.
6. Burbank, J., "Anodization of Lead and Lead Alloys in Sulfuric Acid," J. Electrochem. Soc., *104*, No. 12 (December 1957), pp. 693–701.
7. Schumacher, E. E., "The Nature of Metals in Relation to their Properties," Sci. Monthly, *34* (January 1932), pp. 22–30.
8. Schumacher, E. E., and Bouton, G. M., "Age Hardening Lead Calcium Alloys," Metals and Alloys, *1* (March 1930), pp. 405–409.
9. Simon, A. C., "Stress Corrosion in the Grids of the Lead-Acid Storage Battery," *114*, No. 1 (January 1967), pp. 1–8.
10. Feder, D. O., Koontz, D. E., Babusci, L. D., and Luer, H. J., "Reserve Batteries for Bell System Use: Design of the New Cell," B.S.T.J., this issue, pp. 1253–1278.